Clays and Clay Minerals (2024), **72**, e18, 1–10
doi:10.1017/cmn.2024.30

Original Paper

Microscopic observations of smectite cation exchange in the absence of free water: implications for the evolution of Mars sediments

Christopher Geyer[1], Andrew S. Elwood Madden[1,2], Preston R. Larson[2] and Megan Elwood Madden[1]

[1]School of Geosciences, University of Oklahoma, Norman, OK, USA and [2]Samuel Roberts Noble Microscopy Laboratory, University of Oklahoma, Norman, OK, USA

Abstract

Models of cation exchange mechanisms and driving forces have proven effective predictors of clay behavior and chemistry, but are largely theoretical, particularly in complex systems involving high ionic strength brines or systems where hydration is controlled by relative humidity. In arid and cold environments, such as Mars, cyclical relative humidity variations may play a role in chemical alteration, particularly if clay minerals such as smectite are in the presence of salts. This study examines the effects of relative humidity on smectite-salt mixtures using environmental scanning electron microscopy (ESEM) to observe the physiochemical effects of salt deliquescence and desiccation on smectite textures and elemental distributions. Results demonstrate that even reaction periods as short as a few minutes allow ample time for relative humidity to affect the smectite-salt mixtures. In addition to smectite swelling and salt deliquescence, we also observed rapid changes in element distributions within the smectite and new crystal growth in the presence of high relative humidity. Even in the absence of bulk liquid water, exchangeable cations migrated out of the smectite and formed new crystals at the smectite-salt interface. The observed microscopic changes in elemental distributions indicate that the migration of cations driven by cation exchange led to secondary mineral precipitation, likely a $CaSO_4$ mineral, within a sub-micrometer-thick layer of water on the smectite grains. The results of this study demonstrate that during periods of elevated relative humidity, active smectite mineral alteration and secondary mineral precipitation may be possible on present-day Mars where salts and smectites are in direct physical contact.

Keywords: cation exchange; environmental scanning electron microscopy; Mars; scanning electron microscopy; smectite

(Received: 06 December 2023; revised: 25 July 2024; accepted: 20 August 2024)

Introduction

Clay minerals are ubiquitous across Earth and have also been detected on Mars (Ehlmann and Edwards, 2014; Bishop et al., 2018; Tu et al., 2021b) and other planetary bodies (Rivkin et al., 2006; Ammannito et al., 2016). Clay minerals are also used in many different applications such as environmental remediation and protection, agriculture, and manufacturing and as additives in drilling fluids and paper (Schoonheydt, 2016). Within this study, the term 'clay' is used to refer to a clay mineral, e.g. smectite, rather than a particular grain size. Smectites are known to react with brines and there are many environments where a complex relationship exists between smectites and salts/brines, including evaporitic playa environments (Rosen, 1994) and cold aqueous systems such as Don Juan Pond in Antarctica and sediments on the surface of Mars (Schwenzer et al., 2012; Wilson et al., 2014; Rapin et al., 2019; Tu et al., 2021a). In extremely cold environments, free liquid water is uncommon and increased relative humidity as a result of diurnal or seasonal variations becomes a significant factor when considering water–rock interactions (Polkko et al., 2023). The hygroscopic nature of some salts leads to salt deliquescence during periods of sufficiently elevated relative humidity resulting in interactions between brines and smectite minerals (Brass, 1980; Dickinson and Rosen, 2003; Gough et al., 2014).

Although smectites, and associated cation exchange reactions, have been the focus of intense study for decades, new technology and techniques allow us to observe previously studied phenomena in new ways. One such application is environmental scanning electron microscopy (ESEM) which provides a unique opportunity to observe dynamic reactions in almost real time at micrometer to nanometer scales. Fundamentally, ESEM is an extension of scanning electron microscopy (SEM) in which a high level of vacuum is not required within the sample chamber (Danilatos, 1988; Goldstein et al., 2018). In addition, the researcher can often control the environmental conditions experienced by the sample including precise control of water vapor pressure and temperature in the sample chamber. Therefore, ESEM samples do not experience desiccation as a result of high vacuum and the sample preparation requirements are substantially less complex compared with traditional SEM; in some cases no preparation is required (Baker et al., 1993). Although clays are electrically insulating and typically would experience a charging

Corresponding author: Christopher Geyer; Email: Christopher.Geyer@OU.edu
Cite this article: Geyer C., Elwood Madden A.S., Larson P.R., & Elwood Madden M. (2024). Microscopic observations of smectite cation exchange in the absence of free water: implications for the evolution of Mars sediments. *Clays and Clay Minerals* **72**, e18, 1–10. https://doi.org/10.1017/cmn.2024.30

effect inherent in electron microscopy applications, the presence of water vapor in ESEM applications reduces this charging effect, allowing greater resolution imaging of clays without coating. Accessories such as a Peltier cooling stage allow the researcher to modify experimental conditions *in situ*. By modifying conditions inside the ESEM chamber, dynamic experiments can be conducted while obtaining high-quality microscopic imaging of the reactants and products *in situ*, as the reaction is occurring.

Since the early 1990s, researchers have used ESEM to investigate the effects of relative humidity on smectite swelling, including studies focused on fluid–rock interactions within hydrocarbon reservoirs (Mehta, 1991; Uwins et al., 1993; Baker et al., 1994). Additional studies have examined the effects of clay–water vapor reactions, including efforts to determine the mechanism(s) responsible for damage to ancient Egyptian sculptures stored in a museum. By subjecting sepiolite and palygorskite clays to cyclical wetting and drying cycles, with and without NaCl salt present, Rodriguez-Navarro et al. (1998) confirmed visually that swelling at elevated relative humidities was amplified in the presence of NaCl salt.

Most clay studies using ESEM and varying relative humidity have overwhelmingly focused on clay swelling (Mehta, 1991; Uwins et al., 1993; Baker et al., 1994; Carrier et al., 2013; Sun et al., 2019). However, in the presence of sorbed water or brine formed via salt deliquescence, cation exchange may also occur. Cation exchange is the process by which cations present in an aqueous solution undergo exchange with labile cations in a clay (Grim, 1968). On Mars, diagenetic processes may have included acidic leaching, cation exchange, and limited mass transport due to low water: rock volumes (Vaniman et al., 2011; Yen et al., 2017; Geyer et al., 2023). The effects of cation exchange processes on the smectite and surrounding sediments largely depend on the specific conditions present. A series of previous studies examined relative humidity cycling of smectite-salt mixtures in order to better understand the evolution of $CaSO_4$ and $MgSO_4$ hydrates like those observed on Mars (Vaniman and Chipera, 2006; Vaniman et al., 2011; Wilson and Bish, 2011; Vaniman et al., 2018). The experiments used X-ray diffraction (XRD) to detect sulfate mineral changes as a result of varied relative humidity and found that relative humidity cycling not only affected sulfate mineralogy but that the presence of smectite also had an influence. Wilson and Bish (2011) attributed the appearance of hydrated $CaSO_4$ to cation exchange between deliquesced $MgSO_4$ salts and Ca-bearing smectite in the absence of free liquid water. Although the results of the above-mentioned studies shed light on the relationship between relative humidity and cation exchange, XRD measurements did not allow direct observation of the mechanisms driving cation exchange and the spatial relationships of subsequent secondary minerals. A conceptual model of angstrom-thick briny films reacting with minerals at both Antarctica and on Mars has been proposed by Dickinson and Rosen (2003). By studying ground-ice that forms as pore or fracture filling in soils at Dry Valleys, Antarctica, they demonstrated that the ground-ice was unlikely to be a product of meltwater, instead arguing that deliquescence of salts driven by relative humidity was likely the source of the ground-ice. While the study performed by Dickinson and Rosen is supported by bulk chemical analysis and isotopes of ground-ice, as well as static SEM mineral images, direct evidence linking relative humidity and reactions occurring in Antarctic soils is absent (Dickinson and Rosen, 2003).

The purpose of this study was to investigate the physiochemical effects of relative humidity on smectite-salt mixtures at the microscopic scale using ESEM. Understanding the effects of brine–smectite interactions is important for interpreting mineral assemblages and geomorphology formed in extremely cold aqueous environments, including Don Juan Pond and sedimentary systems on Mars. This study addresses the dearth of microscale, in situ observations of cation exchange reactions by examining the effects of relative humidity on smectite-salt mixtures via ESEM during temperature-driven humidity cycles.

Materials and methods

Experimental overview

In order to evaluate the effects of relative humidity (RH) on smectite particles in contact with salts and the potential for cation exchange, samples were observed using ESEM to collect high resolution secondary electron (SE) images and elemental maps of target smectite particles before, during, and after a 100% RH cycle. Preliminary experiments were conducted to determine optimal sample quantities and imaging parameters, while also defining equipment limitations. From preliminary experiments, 100 mg of sample was determined to be sufficient to prevent the formation of free liquid water within the duration of the experiments. In subsequent experiments, the sample quantity was increased to 2 g, and the time spent at 100% RH was reduced in order to prevent the formation of free liquid water.

Montmorillonite 'SAz-1' (Apache County, AZ, USA) from the Source Clays Repository of The Clay Mineral Society was used as the clay substrate in these experiments because it has been characterized extensively (Xu et al., 2000; Chipera and Bish, 2001; Mermut and Cano, 2001; Mermut and Lagaly, 2001) and allows direct comparison with results of previous studies (Wilson and Bish, 2011; 2012). SAz-1 is a 2:1 phyllosilicate dioctahedral smectite ($Na_{0.4}(Al_{1.6}Mg_{0.4})Si_4O_{10}(OH)_2$) with a relatively high cation exchange capacity (CEC) at 123 meq 100 g^{-1} (Borden and Giese, 2001; Essington, 2015). As with many 2:1 phyllosilicates, SAz-1 exhibits remarkable swelling when exposed to water, either as free liquid or vapor. This swelling is the result of water molecules sorbing between adjacent 2:1 layers; the water molecules may contribute to hydration of interlayer cations or be present as discrete layers of water in addition to the hydrated interlayer cations (Grim, 1968; Moore and Reynolds, 1997)

To create a consistent starting material, natural SAz-1 was soaked in saturated $CaCl_2$ solution for >24 h to replace all exchangeable cations with Ca^{2+}. The SAz-1 was then separated from the liquid by three rounds of centrifugation for 20 min at 10,000 rpm and rinsed with 18.2 MΩ-cm H_2O, followed by freeze drying and gentle homogenization in a mortar and pestle. SAz-1 was mixed with ACS grade (>99.0% purity) Na_2SO_4 or $MgSO_4$ anhydrous salts in a 1:10 salt:montmorillonite mass ratio. To form direct contacts between salt and montmorillonite grains as well as minimize air-filled pockets within the sample, a custom 3D-printed sample press was developed. This allowed uniform compression of the sample while conforming to the dimensions of the sample cup; by pressing the air out of the sample during sample preparation, minimal decompression occurred during the initial vacuum conditions inside the ESEM sample chamber. In addition, the sample press produced a relatively flat surface on the sample which made it significantly easier to image in the microscope. After the sample was mixed and pressed it was immediately loaded into the ESEM chamber.

Na_2SO_4 and $MgSO_4$ salts were chosen because: (1) they have been observed on Mars (Hecht et al., 2009); and (2) the deliquescence

https://doi.org/10.1017/cmn.2024.30 Published online by Cambridge University Press

points of both are well known and are within the range of relative humidity observed on present-day Mars. Therefore, they may have served an important role in Martian rheological and diagenetic processes (Brass, 1980; Vaniman et al., 2004; Möhlmann and Thomsen, 2011). Using two different salts also allowed us to compare the effects of cation chemistry on deliquescence and cation exchange behavior. Generally, for electrolyte solutions with low cation concentrations mixed with montmorillonite, cation selectivity preferences of montmorillonite follow Ca^{2+}>Mg^{2+}>Na^{+}, where Ca^{2+} is retained in the montmorillonite interlayer most strongly and Na^{+} is most weakly retained in the montmorillonite (Sposito et al., 1983a; Tang and Sparks, 1993; Appelo and Postma, 2004). However, when the electrolyte solution is not dilute, but instead the cation in solution is at such a high concentration as to be considered near-infinite, montmorillonite cation selectivity plays a less significant role. Instead, the dominant influence of which cation is adsorbed in the montmorillonite interlayer is controlled by the law of mass action. If, for example, a Ca^{2+}-saturated montmorillonite was mixed with a near-saturated Na_2SO_4 solution, then some of the adsorbed Ca^{2+} cations would exchange with the Na^{+} cations in solution (Sposito et al., 1983b). Following the exchange, the Ca^{2+} now in solution could complex with the available SO_4^{2-}, potentially leading to precipitation of $CaSO_4$ minerals such as gypsum ($CaSO_4 \cdot 2H_2O$), basanite ($CaSO_4 \cdot \frac{1}{2}H_2O$), and anhydrite ($CaSO_4$).

Scanning electron microscopy

Imaging and analysis were accomplished using a ThermoFisher Scientific Quattro S field emission ESEM with a 20 kV accelerating voltage and a probe current of 4.1 mA; working distance varied depending on vacuum conditions. High-resolution SE images were collected at a chamber pressure of 70 Pa with a gaseous secondary electron detector operating in the secondary electron mode. Elemental analysis and mapping were accomplished using energy dispersive X-ray spectroscopy (EDS) in both high-vacuum and low-vacuum ESEM conditions. RH within the chamber was controlled by holding the chamber water vapor pressure constant at 800 Pa and cooling or heating the sample to a target temperature using a Peltier cold stage. The target temperature for a desired RH% was determined using the Antoine equation with updated parameters (NIST: https://webbook.nist.gov/cgi/cbook.cgi?ID=C7732185&Units=SI&Type=ANTOINE&Plot; Wood, 1970); temperatures during the relative humidity cycles varied between 25.2°C and 3.8°C. Starting RH was ~3% and was increased to 100% RH over a period of 30 min, 100% RH was maintained for 1 h followed by a ramp back to ~3% RH over 30 min. Three per cent RH was chosen as the starting RH because this RH could be easily maintained in high-vacuum mode, allowing high-resolution imaging and X-ray analysis prior to and after exposure to 100% RH. In some cases, images of the montmorillonite particles are only presented after the RH ramp due to movement of the sample and loss of the original location.

Results

Initial montmorillonite characterization

The SAz-1 after Ca-saturation was fine grained with aggregates of montmorillonite particles averaging between 5 and 12 μm in diameter (Fig. 1). EDS elemental mapping prior to reaction confirmed that Ca was distributed homogeneously throughout the starting material. Magnesium was also abundant in SAz-1, likely in the octahedral sheet as noted elsewhere (Essington, 2015; Mermut and Cano, 2001; Moore and Reynolds, 1997) (Fig. 2).

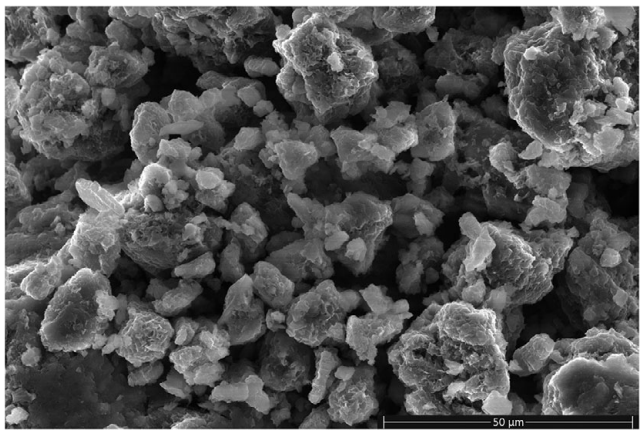

Figure 1. SE image of the unaltered montmorillonite starting material.

Preliminary experiment

A preliminary test was conducted to determine optimal sample conditions as well as identify the potential impact of equipment limitations. In the preliminary experiment ~100 mg of Na_2SO_4 salt +smectite was used to test the hypothesis that elevated RH within the instrument chamber would produce free bulk water in contact with the sample.

As expected, one of the most recognizable processes observed during the relative humidity cycling was swelling. In every experiment, as relative humidity increased, SAz-1 particles increased in diameter with a concurrent loss or reduction in sharpness of angular features; as relative humidity decreased, the same particles shrank in diameter and angular features regained their sharpness. Below 25% RH, no smectite volumetric changes were observed; any apparent sample shifting at <25% RH was attributed to thermal equilibration. Once RH increased beyond 25%, montmorillonite particles began to swell and shift, with individual montmorillonite particles increasing in diameter and roundness in real-time. While the montmorillonite particles equilibrated quickly (<30 s) at any given RH, the salt crystals took much longer to equilibrate. In many cases, it took >2 min for salt crystals to become visibly affected by the humidity, although the time was heavily dependent on the volume of the salt crystals.

Secondary electron images were collected throughout the hydration-dehydration cycles. In Fig. 3A, the sample was equilibrated at 25% RH and no bulk liquid water was observed. As the salt crystal equilibrated at 100% RH, roughening of the salt crystal surfaces became apparent (Fig. 3B), then as RH was held constant at 100%, a uniform layer of liquid formed, first on the Na_2SO_4 surfaces and eventually engulfed the montmorillonite particles (Fig. 3C). The bulbous, nodular shapes shown on the Na_2SO_4 crystal face in Fig. 3C were interpreted as a homogeneous water layer rather than a solid. As the RH increased, the nodules grew laterally and vertically like a film. Eventually, this nodular film grew to the point where it came into visible contact with the montmorillonite grains and began to cover them. Finally, as RH was brought back down to 25% the film covering the surfaces shrank in a similar manner to the growth stage, but in the reverse direction as RH decreased. The remaining bulk liquid water flash evaporated or co-precipitated at a

https://doi.org/10.1017/cmn.2024.30 Published online by Cambridge University Press

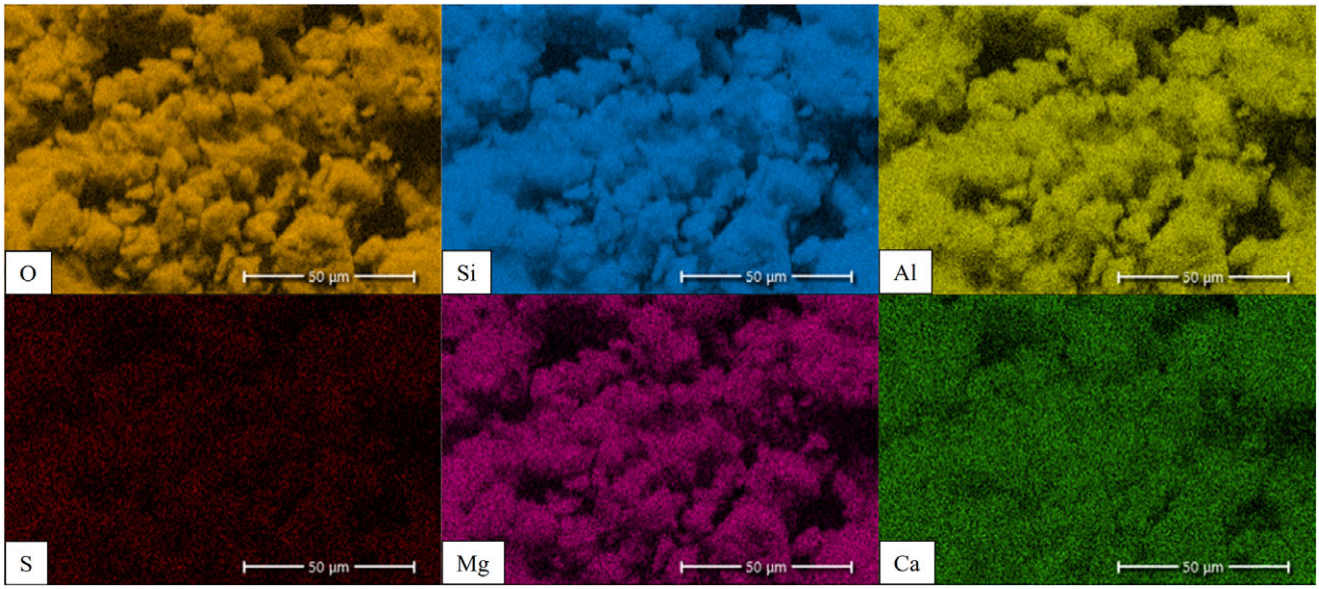

Figure 2. Colorized EDS X-ray maps of the unaltered montmorillonite under initial conditions, from the same area as Fig. 1. Color intensity is proportional to the concentration of the indicated element at each pixel (Na and Fe also detected but not shown).

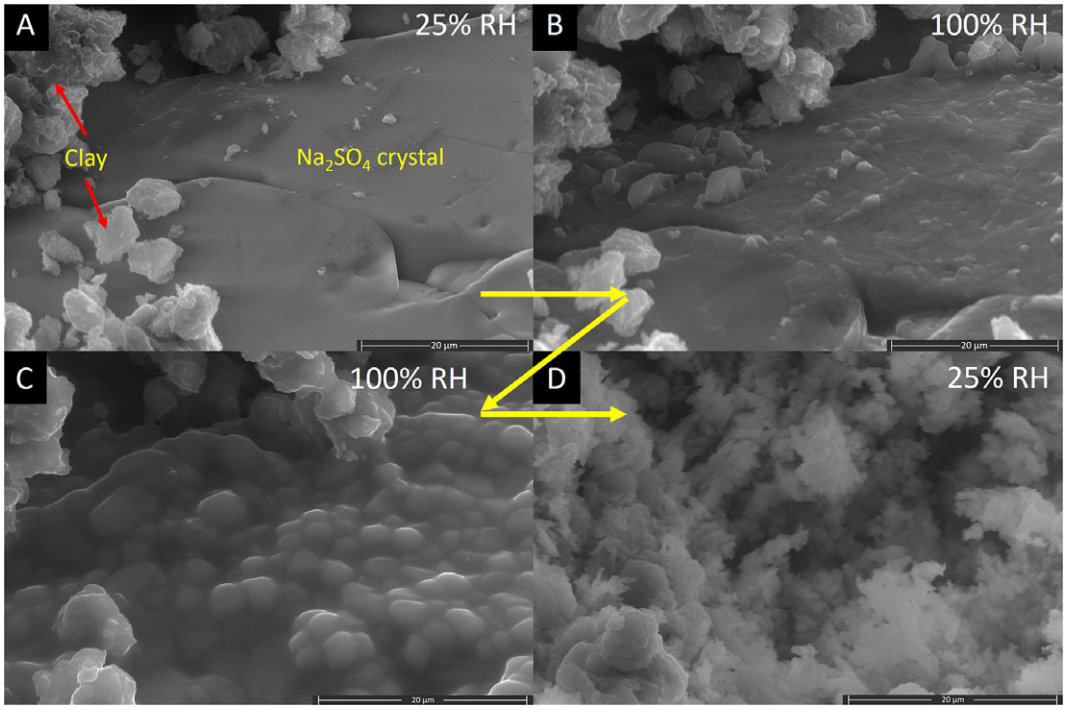

Figure 3. SAz-1 on a Na_2SO_4 crystal with yellow arrows indicating the progression through one humidity cycle, starting at A and finishing at D. (A) 25% RH prior to exposure to elevated RH. (B) 100% RH after 30 min, observable montmorillonite swelling and increased surface roughness of the Na_2SO_4 crystal face. (C) 100% RH after 2.5 h, montmorillonite swelling had ceased, yet clear edges and particle shapes were maintained in the montmorillonite particles. No distinct features of the Na_2SO_4 crystal remained. Instead, the salt was covered with a bulbous, nodular film. (D) Return to 25% RH after 2.5 h at 100% RH, a network of nano- to micro-scale crystals, likely re-crystallized Na_2SO_4 appeared, no further changes were observed after return to 3% RH.

point between 28% RH and 24% RH, leaving behind a network of nano- to microscale material that likely formed from widespread dissolution–precipitation (Fig. 3D).

It is important to note the presence of a thick layer of bulbous material, which we interpret as bulk liquid water, visible in Fig. 3C. We hypothesize that the small sample volume and extended time at 100% RH in the preliminary experiment allowed a layer of bulk water to accumulate. However, in subsequent experiments no bulk water was observed, likely due to the larger sample volumes and reduced time spent at 100% RH. These subsequent experiments were performed using fresh, unreacted salt-montmorillonite mixtures.

https://doi.org/10.1017/cmn.2024.30 Published online by Cambridge University Press

Na_2SO_4 experiments in the absence of bulk water

A clear area with montmorillonite particles or isolated aggregates in contact with a Na_2SO_4 crystal were identified in order to study montmorillonite–salt interactions in situ (Fig. 4). The Na_2SO_4 crystal and montmorillonite composition was confirmed using EDS and detailed images collected before and after exposure to 100% RH (Target Grain 1: 'TG1'; Figs 4–6). As humidity increased to 100% RH, significant lateral and vertical motion of the sample was observed, which was attributed to montmorillonite swelling due to increased hydration of the interlayer cations and/or additional interlayer water layers (Slade et al., 1991). However, at no point during the relative humidity cycle was liquid water observed, even at 100% RH. Significant alteration of both the salt and montmorillonite were observed, however, most notably the formation of a salt dissolution pit which formed around a montmorillonite particle shown in Fig. 4B.

After exposing the sample to 100% RH and then decreasing RH back to ~3%, new crystals appeared where montmorillonite particles were in contact with the Na_2SO_4 salt. It is worth noting that the new crystals only occurred where the montmorillonite was in direct contact with the salt; portions of the montmorillonite which were physically distant from the salt showed no signs of crystal nucleation or alteration other than residual swelling (Fig. 5). Large portions of the Na_2SO_4 crystal face also appeared to have been etched, particularly around TG1, but also around some of the other montmorillonite grains. One particularly notable dissolution pit surrounding TG1 had an indentation that mirrored the growth of the crystal attached to TG1 (just above the red rectangle in Fig. 4B). Additionally, the vertical topographic trench that crosses vertically through the field of view is visibly wider after 100% RH exposure.

In addition to evidence of etching and dissolution, new crystals also appeared after exposure to 100% RH. These new crystals exhibited completely different crystal habit relative to the Na_2SO_4 salt and also had a different chemical composition. EDS elemental mapping (Fig. 6) showed before and after element maps of TG1. Prior to the 100% RH ramp, Ca was distributed homogeneously in TG1; however, after reaching 100% RH, the Ca appeared to migrate from the center of the montmorillonite to the new crystals which formed at the contact between the montmorillonite and the Na_2SO_4

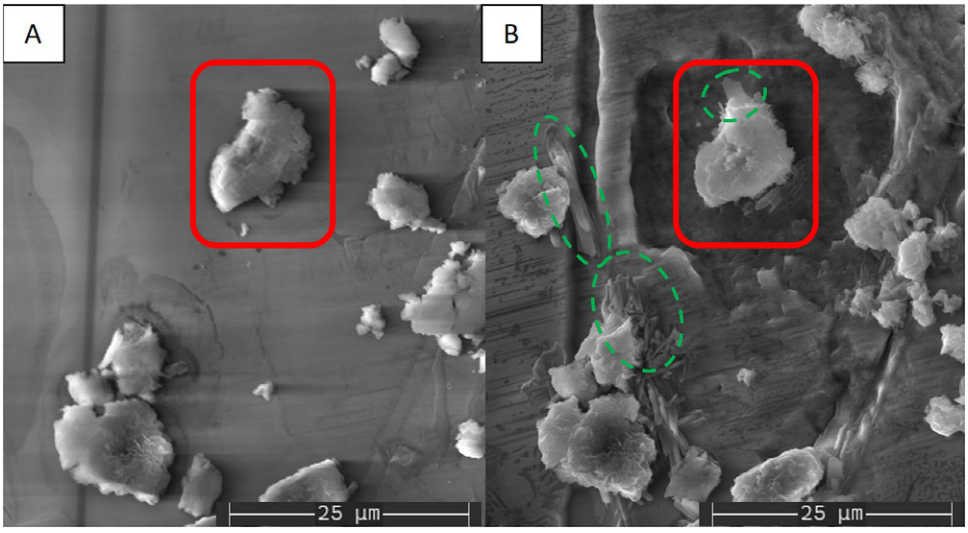

Figure 4. SE images of the target site consisting of montmorillonite clumps lying on top of a Na_2SO_4 crystal face, red boxes in panels A and B highlighting Target Grain 1 (TG1). (A) Initial conditions. (B) After exposure to 100% RH, severe dissolution etching and crystal formation were observed; the dashed green ovals highlight secondary crystals further detailed in Fig. 5.

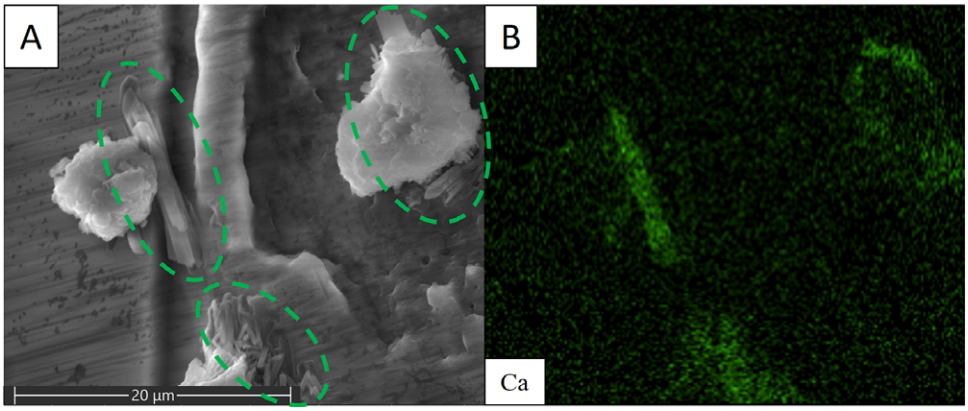

Figure 5. Close-up of new crystals depicted in Fig. 4B, TG1 present at top right of both images. (A) SE image, green dashed ovals indicate new crystals. (B) Color EDS image of Ca for the same area as Fig. 4A. Note the presence of SAz-1 grains visible in the SE image but undetectable by Ca EDS, indicating that Ca has migrated out of the SAz-1 grains and into the surrounding secondary salt crystals precipitated on the surface of the montmorillonite.

https://doi.org/10.1017/cmn.2024.30 Published online by Cambridge University Press

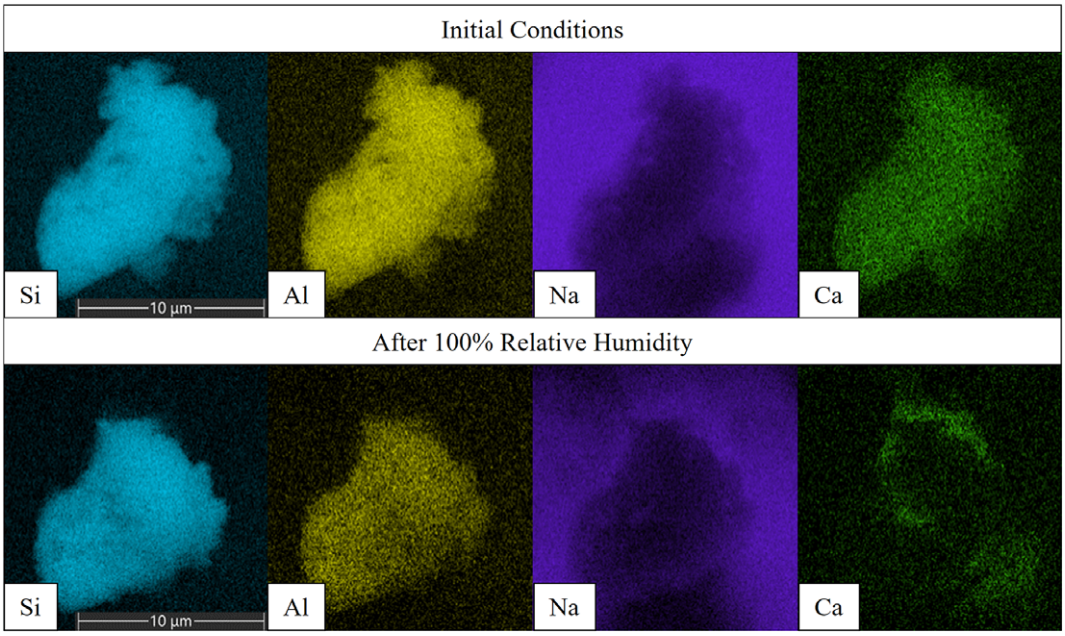

Figure 6. Ca migration observed by comparing before and after color EDS mapping of TG1. The top row images were collected prior to 100% RH, the bottom row images were collected after the sample was exposed to 100% RH and returned to ~3% RH.

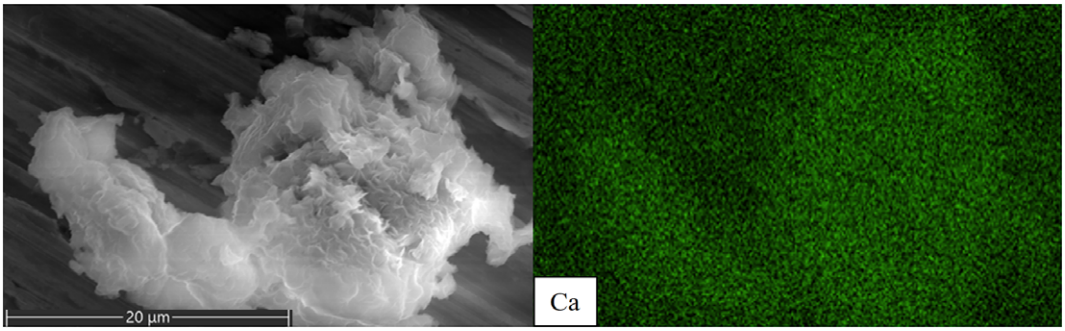

Figure 7. An isolated montmorillonite grain located on the aluminum sample holder wall away from any Na_2SO_4 salt. SE image (left) and color EDS – Ca image (right) collected after the grain was exposed to 100% RH. Note the homogeneous distribution of Ca in the sample.

crystal. Unfortunately, crystal nucleation and growth occurred too rapidly to capture images of growth dynamics.

SAz-1 grains that were isolated from the Na_2SO_4 failed to produce new crystals and the Ca distribution remained homogeneous throughout the experiment (Fig. 7). However, these isolated montmorillonite clumps did exhibit signs of swelling.

$MgSO_4$+SAz-1 interactions

When the montmorillonite was mixed with $MgSO_4$, changes similar to those observed in the SAz-1+Na_2SO_4 experiments occurred. However, in the $MgSO_4$ experiments, greater movement of the montmorillonite–salt mixture occurred as the relative humidity decreased. This prevented the collection of images and elemental maps from being compared directly with the same particle with initial conditions. Luckily, montmorillonite grains that had been in contact with salt crystals during the RH cycle were ubiquitous, allowing interpretation of reactions which occurred as a result of exposure to elevated relative humidity.

Similar to the Na_2SO_4 experiments, EDS elemental maps and SE images of TG2+$MgSO_4$ were collected before and after RH cycling. Like the Na_2SO_4 experiments, blade-like crystals that contained high concentrations of Ca and S, but did not contain abundant Al or Si, appeared after the RH cycle, indicating that the newly formed Ca-rich crystals were related to, but not part of, the SAz-1 particle (Figs 8 and 9).

Discussion

Cation exchange and elemental migration

In both the Na_2SO_4 and $MgSO_4$ experiments, Ca appeared to be concentrated in new crystals observed adjacent to montmorillonite grains (Figs 5 and 9), but only when the montmorillonite grains were in contact with salt crystals during a RH cycle. Ca was homogeneously distributed within montmorillonite grains prior to the relative humidity cycles with salts present (Fig. 2), while after the cycle Ca was no longer homogeneously distributed within the montmorillonite grain (Figs 6 and 9). This migration of Ca coincides with a co-localized concentration of sulfur (Figs 8 and 9),

https://doi.org/10.1017/cmn.2024.30 Published online by Cambridge University Press

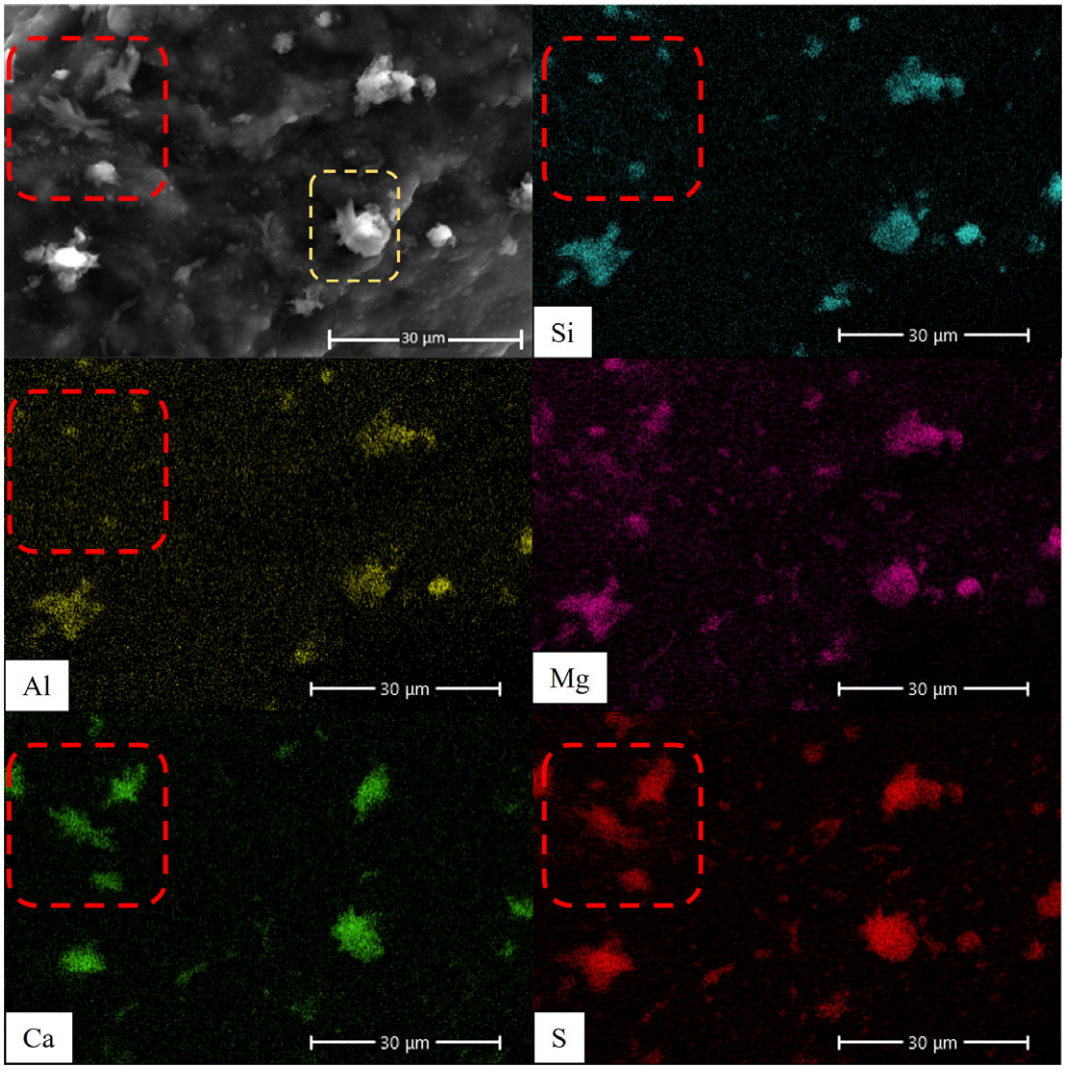

Figure 8. Elemental distributions in SAz-1+$MgSO_4$ after one RH cycle. The red dashed boxes highlight crystals that exhibited co-localized Ca and S, but were lacking in Al or Si. The yellow dashed box in the SE image highlights TG2 shown in Fig. 9.

likely due to growth of $CaSO_4$ crystals at the interface between the salt and the montmorillonite grains. Similar $CaSO_4$ precipitation has been previously observed in XRD experiments investigating smectite-salt interactions during relative humidity changes (Wilson and Bish, 2011; Wilson and Bish, 2012). Based on this co-localization of S and Ca, the Na_2SO_4 and $MgSO_4$ salts likely deliquesced forming a sub-micron layer of brine that facilitated cation exchange between the Ca^{2+} present in the montmorillonite interlayers and the cations in the salts. The exchange of Ca^{2+} from the montmorillonite interlayers resulted in saturation and precipitation of $CaSO_4$, while Na^+ or Mg^{2+} would have migrated from the salt into the montmorillonite to maintain the montmorillonite layer charge neutrality. Element migration with no liquid water observable, even at the sub-micrometer scale, also corroborates the work of Wilson and Bish (2011) that indicated cation exchange can occur even within a molecular-scale surficial water layer.

Applications on Mars

Recurring slope lineae (RSL) observed on Mars, as well as water tracks seen at Don Juan Pond, may not only be indicative of fluid transport but also chemical alteration, albeit on a microscopic scale. While hypotheses differ regarding the cause(s) of RSL, such as if liquid water is present, one explanation is the deliquescence of salts during periods of high relative humidity (Dickson et al., 2013; Gough et al., 2017). Studies examining the water source for Don Juan Pond concluded that flows similar to RSL observed on Mars are likely due to the relative humidity controlled deliquescence of salts (Dickson et al., 2013; Gough et al., 2017). Tu et al. (2021a) found that the presence of elevated Ca^{2+} concentrations in brines at Don Juan Pond is also likely due to cation exchange. When exposed to solutions with sufficient Na^+ concentrations, some smectites will release Ca^{2+} in exchange for Na^+ (McBride, 1980; Toner and Sletten, 2013; Tu et al., 2021a), even though the smectite present at that location would theoretically retain Ca^{2+} preferentially over Na^+.

A common contention to the briny RSL origin hypothesis is that RSL do not correlate perfectly with conditions conducive to the presence of liquid water (see McEwen et al., 2011; Toner et al., 2022, and references within both for a review). Toner et al. (2022) argued against cation exchange as the mechanism for RSL at both Don Juan Pond and on Mars due to the preferential adsorption of Ca^{2+} by smectites when exposed to dilute solutions containing the cations in

https://doi.org/10.1017/cmn.2024.30 Published online by Cambridge University Press

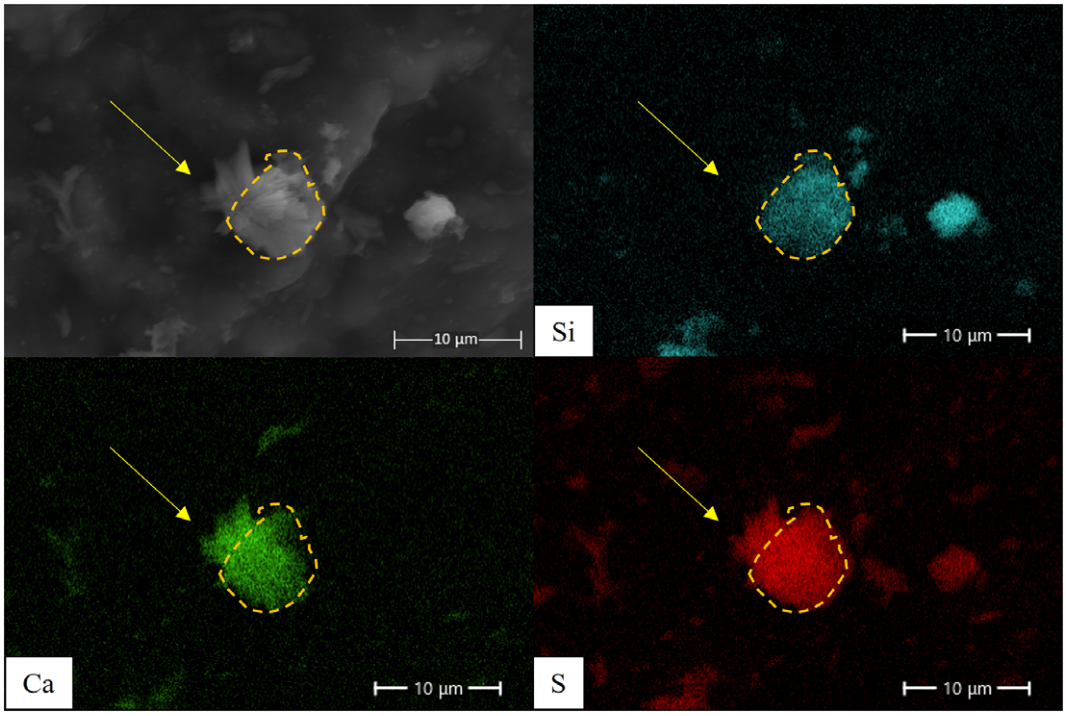

Figure 9. Close-up of TG2 showing differences in elemental distribution; yellow arrows indicate the location of crystals on the upper left of the particle, visible in SE, which contain abundant Ca and S based on the EDS maps, but are absent in the Si EDS map. The yellow dashed polygon outlines the montmorillonite grain as defined by the Si EDS map.

question. However, as demonstrated by the result in the present study, when brine formation is initiated by deliquescence of salts controlled by relative humidity, Ca can migrate out of the smectite interlayer via cation exchange and even mass transport is possible, albeit on a microscopic scale.

The occurrence of cation exchange outside typical boundary conditions that assume bulk liquid water must be present brings with it the realization that Martian sediments may in fact be undergoing active diagenesis at the microscopic scale, even under traditionally 'dry' conditions. For example, hydrated salts have been detected at several RSL locations on Mars (Ojha et al., 2015). Heinz et al. (2016) observed that a Mars analogue soil, when exposed to elevated RH, would only show darkening similar to RSL if salts were present and permitted to deliquesce. Thus, observations of RSL on Mars suggest chemical alteration may be occurring on diurnal and seasonal time scales. Similarly, cation exchange in high-salinity fluids may also have contributed to large $CaSO_4$ concentrations observed across Mars soils, including $CaSO_4$-rich veins (McLennan et al., 2014; Rampe et al., 2020). The elemental composition of sediments at Gale crater suggests limited chemical transport and low water:rock volumes (Bristow et al., 2015); these observations are consistent with the hypothesis that cation exchange played a major role in the formation of the $CaSO_4$ minerals.

Conclusions

ESEM observations revealed how minerals are altered or formed as a direct result of exposure to elevated RH. The results of the present study include a before and after set of SE and elemental images which document the dissolution of salt in the absence of free liquid water, which corresponds with elemental migration consistent with cation exchange between a brine and montmorillonite grains. New crystal formation observed in SE images was further distinguished by collocated concentrations of Ca and sulfur observed in elemental EDS maps, suggesting the formation of a $CaSO_4$-rich phase. In the case of both Na_2SO_4 and $MgSO_4$ salts, after a single RH cycle, montmorillonite grains that had been saturated with Ca and were in direct physical contact with salt grains no longer exhibited a homogeneous Ca distribution. Instead, Ca appeared to migrate to the edge of the grain and into the newly formed crystals. The results of this study thus provide evidence that sub-micrometer thick layers of brine formed by salt deliquescence can facilitate cation exchange and subsequent mineral formation in extreme environments such as Antarctica or Mars.

Author contributions. Christopher Geyer conceived, planned, and executed the experiments under the guidance of Megan Elwood Madden, Andrew S. Elwood Madden, and Preston R. Larson. Preston R. Larson guided instrument operation and image acquisition. Megan Elwood Madden and Andrew S. Elwood Madden supervised data interpretation. All authors provided quality feedback and significantly influenced the research and manuscript.

Acknowledgements. We thank the editors of *Clays and Clay Minerals* as well as three anonymous reviewers for feedback that improved the manuscript.

Financial support. This project was funded by the University of Oklahoma and NASA Solar System Workings Grant 80NSSC23K0037.

Competing interests. The authors declare that they have no competing interests.

Data availability statement. Images used in this research are available upon request

References

Ammannito, E., DeSanctis, M., Ciarniello, M., Frigeri, A., Carrozzo, F., Combe, J.-P., … & Raponi, A. (2016). Distribution of phyllosilicates on the surface of Ceres. *Science*, *353*, aaf4279.

Appelo, C.A.J., & Postma, D. (2004). *Geochemistry, Groundwater and Pollution*. CRC Press.

Baker, J., Uwins, P., & Mackinnon, I. D. (1993). ESEM study of illite/smectite freshwater sensitivity in sandstone reservoirs. *Journal of Petroleum Science and Engineering*, *9*, 83–94.

Baker, J., Uwins, P., & Mackinnon, I.D. (1994). Freshwater sensitivity of corrensite and chlorite/smectite in hydrocarbon reservoirs – an ESEM study. *Journal of Petroleum Science and Engineering*, *11*, 241–247.

Bishop J.L., Fairén A.G., Michalski J.R., Gago-Duport L., Baker L.L., Gross C., Velbel M.A., & Rampe E.B. (2018). Surface clay formation during short-term warmer and wetter conditions on a largely cold ancient Mars. *Nature Astronomy*, *2*, 206–213.

Borden, D., & Giese, R. (2001). Baseline studies of the clay minerals society source clays: cation exchange capacity measurements by the ammonia-electrode method. *Clays and Clay Minerals*, *49*, 444–445.

Brass, G.W. (1980). Stability of brines on Mars. *Icarus*, *42*, 20–28. doi: 10.1016/0019-1035(80)90237-7

Bristow, T.F., Bish, D.L., Vaniman, D.T., Morris, R.V., Blake, D.F., Grotzinger, J. P., … & Ming, D.W. (2015). The origin and implications of clay minerals from Yellowknife Bay, Gale crater, Mars. *American Mineralogist*, *100*, 824–836.

Carrier, B., Wang, L., Vandamme, M., Pellenq, R.J.-M., Bornert, M., Tanguy, A., & Van Damme, H. (2013). ESEM study of the humidity-induced swelling of clay film. *Langmuir*, *29*, 12823–12833.

Chipera, S.J., & Bish, D.L. (2001). baseline studies of the Clay Minerals Society source clays: powder X-ray diffraction analyses. *Clays and Clay Minerals*, *49*, 398–409. doi: 10.1346/CCMN.2001.0490507

Danilatos, G. (1988). Foundations of environmental scanning electron microscopy. In *Advances in Electronics and Electron Physics* (vol. *71*, pp. 109–250). Elsevier.

Dickinson, W.W., & Rosen, M.R. (2003). Antarctic permafrost: an analogue for water and diagenetic minerals on Mars. *Geology*, *31*, 199–202.

Dickson, J.L., Head, J.W., Levy, J.S., & Marchant, D.R. (2013). Don Juan Pond, Antarctica: near-surface $CaCl_2$-brine feeding Earth's most saline lake and implications for Mars. *Scientific Reports*, *3*, 1–8.

Ehlmann, B.L., & Edwards, C.S. (2014). Mineralogy of the Martian surface. *Annual Review of Earth and Planetary Sciences*, *42*, 291–315. doi: 10.1146/annurev-earth-060313-055024

Essington, M.E. (2015). *Soil and Water Chemistry: An Integrative Approach*. CRC Press.

Geyer, C., Madden, A.S.E., Rodriguez, A., Bishop, J.L., Mason, D., & Madden, M. E. (2023). The role of sulfate in cation exchange reactions: applications to clay–brine interactions on Mars. *The Planetary Science Journal*, *4*, 48.

Goldstein, J.I., Newbury, D.E., Michael, J.R., Ritchie, N.W., Scott, J.H.J., Joy, D.C., … & Ritchie, N.W.(2018). Attempting electron-excited X-ray microanalysis in the variable pressure scanning electron microscope (VPSEM). *Scanning Electron Microscopy and X-Ray Microanalysis*, 441–459.

Gough, R., Chevrier, V., & Tolbert, M. (2014). Formation of aqueous solutions on Mars via deliquescence of chloride–perchlorate binary mixtures. *Earth and Planetary Science Letters*, *393*, 73–82.

Gough, R., Wong, J., Dickson, J., Levy, J., Head, J., Marchant, D., & Tolbert, M. (2017). Brine formation via deliquescence by salts found near Don Juan Pond, Antarctica: Laboratory experiments and field observational results. *Earth and Planetary Science Letters*, *476*, 189–198.

Grim, R.E. (1968). *Clay Mineralogy* (2nd edn). McGraw-Hill.

Hecht, M. H., Kounaves, S. P., Quinn, R., West, S. J., Young, S. M., Ming, D. W., … & Hoffman, J. (2009). Detection of perchlorate and the soluble chemistry of martian soil at the Phoenix lander site. *Science*, *325*, 64–67.

Heinz, J., Schulze-Makuch, D., & Kounaves, S.P. (2016). Deliquescence-induced wetting and RSL-like darkening of a Mars analogue soil containing various perchlorate and chloride salts. *Geophysical Research Letters*, *43*, 4880–4884.

McBride, M. (1980). Interpretation of the variability of selectivity coefficients for exchange between ions of unequal charge on smectites. *Clays and Clay Minerals*, *28*, 255–261.

McEwen, A.S., Ojha, L., Dundas, C.M., Mattson, S.S., Byrne, S., Wray, J.J., … & Gulick, V.C. (2011). Seasonal flows on warm Martian slopes. *Science*, *333*, 740–743.

McLennan, S.M., Anderson, R., Bell III, J., Bridges, J.C., Calef III, F., Campbell, J. L., … & Cousin, A. (2014). Elemental geochemistry of sedimentary rocks at Yellowknife Bay, Gale crater, Mars. *Science*, *343*, 1244734.

Mehta, S. (1991). *Imaging of wet specimens in their natural state using environmental scanning electron microscope (ESEM): some examples of importance to petroleum technology.* Paper presented at the SPE Annual Technical Conference and Exhibition.

Mermut, A.R., & Cano, A.F. (2001). Baseline studies of the Clay Minerals Society source clays: chemical analyses of major elements. *Clays and Clay Minerals*, *49*, 381–386.

Mermut, A.R., & Lagaly, G. (2001). Baseline studies of the Clay Minerals Society Source Clays: layer-charge determination and characteristics of those minerals containing 2:1 layers. *Clays and Clay Minerals*, *49*, 393–397. doi: 10.1346/CCMN.2001.0490506

Möhlmann, D., & Thomsen, K. (2011). Properties of cryobrines on Mars. *Icarus*, *212*, 123–130.

Moore, D.M., & Reynolds, R.C., Jr (1997). *X-Ray Diffraction and the Identification and Analysis of Clay Minerals* (2nd edn). Oxford University Press.

Ojha, L., Wilhelm, M. B., Murchie, S. L., McEwen, A. S., Wray, J. J., Hanley, J., … & Chojnacki, M. (2015). Spectral evidence for hydrated salts in recurring slope lineae on Mars. *Nature Geoscience*, *8*, 829–832.

Polkko, J., Hieta, M., Harri, A. M., Tamppari, L., Martínez, G., Viúdez-Moreiras, D., … & De La Torre Juarez, M. (2023). Initial results of the relative humidity observations by MEDA instrument onboard the Mars 2020 Perseverance Rover. *Journal of Geophysical Research: Planets*, *128*, e2022JE007447.

Rampe, E.B., Blake, D.F., Bristow, T., Ming, D.W., Vaniman, D., Morris, R., … & Tu, V. (2020). Mineralogy and geochemistry of sedimentary rocks and eolian sediments in Gale crater, Mars: a review after six Earth years of exploration with Curiosity. *Geochemistry*, *80*, 125605.

Rapin, W., Ehlmann, B.L., Dromart, G., Schieber, J., Thomas, N., Fischer, W.W., … & Clark, B.C. (2019). An interval of high salinity in ancient Gale crater lake on Mars. *Nature Geoscience*, *12*, 889–895.

Rivkin, A., Volquardsen, E., & Clark, B. (2006). The surface composition of Ceres: discovery of carbonates and iron-rich clays. *Icarus*, *185*, 563–567.

Rodriguez-Navarro, C., Sebastian, E., Doehne, E., & Ginell, W.S. (1998). The role of sepiolite-palygorskite in the decay of ancient Egyptian limestone sculptures. *Clays and Clay Minerals*, *46*, 414–422.

Rosen, M.R. (1994). The importance of groundwater in playas: a review of playa classifications and the sedimentology and hydrology of playas. In *Paleoclimate and Basin Evolution of Playa Systems* (pp. 1–18). Geological Society of America.

Schoonheydt, R.A. (2016). Reflections on the material science of clay minerals. *Applied Clay Science*, *131*, 107–112.

Schwenzer, S., Abramov, O., Allen, C., Bridges, J., Clifford, S., Filiberto, J., … & Newsom, H. (2012). Gale crater: formation and post-impact hydrous environments. *Planetary and Space Science*, *70*, 84–95.

Slade, P., Quirk, J., & Norrish, K. (1991). Crystalline swelling of smectite samples in concentrated NaCl solutions in relation to layer charge. *Clays and Clay Minerals*, *39*, 234–238.

Sposito, G., Holtzclaw, K. M., Charlet, L., Jouany, C., & Page, A. (1983a). Sodium-calcium and sodium-magnesium exchange on Wyoming bentonite in perchlorate and chloride background ionic media. *Soil Science Society of America Journal*, *47*, 51–56.

Sposito, G., Holtzclaw, K.M., Jouany, C., & Charlet, L. (1983b). Cation selectivity in sodium-calcium, sodium-magnesium, and calcium-magnesium exchange on Wyoming bentonite at 298 K. *Soil Science Society of America Journal*, *47*, 917–921.

Sun, H., Mašín, D., Najser, J., Neděla, V., & Navrátilová, E. (2019). Bentonite microstructure and saturation evolution in wetting–drying cycles evaluated using ESEM, MIP and WRC measurements. *Géotechnique*, *69*, 713–726.

Tang, L., & Sparks, D.L. (1993). Cation-exchange kinetics on montmorillonite using pressure-jump relaxation. *Soil Science Society of America Journal*, *57*, 42–46.

Toner, J., Sletten, R., Liu, L., Catling, D., Ming, D., Mushkin, A., & Lin, P.-C. (2022). Wet streaks in the McMurdo Dry Valleys, Antarctica: implications for recurring slope lineae on Mars. *Earth and Planetary Science Letters*, *589*, 117582.

https://doi.org/10.1017/cmn.2024.30 Published online by Cambridge University Press

Toner, J.D., & Sletten, R.S. (2013). The formation of Ca-Cl-rich groundwaters in the Dry Valleys of Antarctica: field measurements and modeling of reactive transport. *Geochimica et Cosmochimica Acta*, *110*, 84–105.

Tu, V.M., Ming, D., & Sletten, R. (2021a). The mineralogy and cation exchange of sediments in Don Juan Pond, Antarctica Dry Valley: implications for Mars. *LPI Contributions*, *2614*, 6021.

Tu, V.M., Rampe, E.B., Bristow, T.F., Thorpe, M.T., Clark, J.V., Castle, N., … Bedford, C. (2021b). A review of the phyllosilicates in Gale crater as detected by the CheMin instrument on the Mars Science Laboratory, Curiosity rover. *Minerals*, *11*, 847.

Uwins, P.J., Baker, J.C., & Mackinnon, I.D. (1993). Imaging fluid/solid interactions in hydrocarbon reservoir rocks. *Microscopy Research and Technique*, *25*, 465–473.

Vaniman, D., Bish, D., Chipera, S., & Rearick, M. (2011). *Relevance to Mars of cation exchange between nontronite and Mg-sulfate brine.* Paper presented at the Lunar and Planetary Science Conference.

Vaniman, D.T., Bish, D.L., Chipera, S.J., Fialips, C.I., William Carey, J., & Feldman, W.C. (2004). Magnesium sulphate salts and the history of water on Mars. *Nature*, *431*, 663–665.

Vaniman, D.T., & Chipera, S.J. (2006). Transformations of Mg- and Ca-sulfate hydrates in Mars regolith. *American Mineralogist*, *91*, 1628–1642.

Vaniman, D.T., Martínez, G.M., Rampe, E.B., Bristow, T.F., Blake, D.F., Yen, A.S., … & Morookian, J.M. (2018). Gypsum, bassanite, and anhydrite at Gale crater, Mars. *American Mineralogist: Journal of Earth and Planetary Materials*, *103*, 1011–1020.

Wilson, M., Wilson, L., Patey, I., & Shaw, H. (2014). The influence of individual clay minerals on formation damage of reservoir sandstones: a critical review with some new insights. *Clay Minerals*, *49*, 147–164.

Wilson, S.A., & Bish, D.L. (2011). Formation of gypsum and bassanite by cation exchange reactions in the absence of free-liquid H_2O: implications for Mars. *Journal of Geophysical Research: Planets*, *116*.

Wilson, S.A., & Bish, D.L. (2012). Stability of Mg-sulfate minerals in the presence of smectites: Possible mineralogical controls on H_2O cycling and biomarker preservation on Mars. *Geochimica et Cosmochimica Acta*, *96*, 120–133.

Wood, L.A. (1970). The use of dew-point temperature in humidity calculations. *Journal of Research of the National Bureau of Standards–C. Engineering and Instrumentation C*, *74*, 117–122.

Xu, W., Johnston, C.T., Parker, P., & Agnew, S.F. (2000). Infrared study of water sorption on Na-, Li-, Ca-, and Mg-exchanged (SWy-1 and SAz-1) montmorillonite. *Clays and Clay Minerals*, *48*, 120–131. doi: 10.1346/CCMN.2000.0480115

Yen, A., Ming, D., Vaniman, D., Gellert, R., Blake, D., Morris, R., … & Edgett, K. (2017). Multiple stages of aqueous alteration along fractures in mudstone and sandstone strata in Gale crater, Mars. *Earth and Planetary Science Letters*, *471*, 186–198.

https://doi.org/10.1017/cmn.2024.30 Published online by Cambridge University Press